Influence of the Human Activity on Wide-Band Characteristics of the 60 GHz Indoor Radio Channel

Sylvain Collonge, Gheorghe I. Zaharia, Ghaïs El Zein

Influence of the Human Activity on Wide-Band Characteristics of the 60 GHz Indoor Radio Channel

Sylvain Collonge, *Student Member, IEEE*, Gheorghe Zaharia, and Ghais El Zein

***Abstract*—This paper presents propagation measurements in the presence of human activity for a 60 GHz channel. Series of 40-min-long measurements of the channel impulse response have been recorded with a sampling period of 1.6 ms, for a total duration of about 20 h. During measurements, the human activity (between zero and 15 persons) was observed with a video camera. The obstruction phenomenon due to the human bodies is characterized in duration and amplitude from the propagation characteristics (attenuation, coherence bandwidth) by means of an appropriate method. The results highlight and quantify the problems due to the human activity for high data rate communication systems. When the direct path is shadowed by a person, the attenuation generally increases by more than 20 dB, for a median duration of about 100 ms for an activity of one to five persons and 300 ms for 11–15 persons. Globally, the channel is "unavailable" for about 1% or 2% of the time in the presence of one to five persons. This channel characterization makes it possible to modelize the temporal variations of the 60 GHz channels. The results also give orientations for the design of high data rate communications systems and networks architectures at 60 GHz.**

***Index Terms*—60 GHz, channel sounding, indoor propagation, millimeter waves, time-varying channel.**

I. Introduction

RECENT advances in wireless high data rate systems have conducted to explore higher frequency bands, such as the extremely high frequency band (30–300 GHz). At these frequencies, propagation loss is strong, which is profitable for frequency reuse, and available bandwidths are large, which makes it possible to ensure very high data rates (>100 Mbps). The applications under interest are sometimes referred to as the fifth generation [1] of wireless communications. The channel characterization is an essential step in the design of these future systems, and particularly channel characterization based on measurements. Several published studies of the 60 GHz propagation focus on different aspects of the indoor channel: the influence of antennas directivity [2], [3], the influence of antennas polarization [4], the angles of arrival analysis [5], [6], etc. Nevertheless, the influence of the human activity on the propagation conditions is less analyzed. Yet it is a critical aspect of the millimeter-wave propagation. The published studies rarely present measurement results ([7]: narrow-band measurements at 30 GHz) but generally simulation results [8]–[10].

This paper presents 60 GHz wide-band propagation measurements in the presence of a "natural" human activity. This paper is based on several hours of channel impulse response recordings, within an indoor environment.

In Section II, we present the measurement setup (procedure, equipment, site description). In Section III, the measurement processing is introduced. In Section IV, the results are presented and analyzed. Section V concludes this paper.

II. Measurement Setup

A. Measurement Equipements

1) Channel Sounder: A 60 GHz channel sounder based on the sliding correlation technique was used [11]. This sounder has a 500 MHz bandwidth. The channel impulse response (IR) is evaluated with a 2.3 ns temporal resolution and a 40 dB relative dynamic. The delay observation window can be adjusted up to 1 μs. This window was set to 80 ns for these measurements. As the sliding factor is also adjustable, the measurement duration of one impulse response can be adapted to the temporal variation of the channel. This duration was set to 1.6 ms.

2) Antennas: Four antennas were used: two horns and two patches. The horns have a 22.4 dB gain and a 12° half-power beamwidth (HPBW) in azimuth, and about 10° in elevation. The patches have a gain of about 3 dB and a 60° HPBW both in elevation and azimuth. The vertical polarization was used. Three couples of antennas are defined for transmission (TX) and reception (RX):

- a horn at TX and RX (HH configuration);
- a patch at TX and a horn at RX (PH configuration);
- a patch at TX and RX (PP configuration).

B. Measurement Environments

Measurements were carried out in a large room (12.9×10.3 m) in the Institute of Electronics and Telecommunications of Rennes laboratory (Fig. 1). This room is a working place with desk and computers. In the upper left corner is the coffee area where researchers usually take a break. A varied human activity can be observed in this corner of the room during precise moments in the daytime. The furniture is composed of a wooden table, chairs with metallic legs, a wooden cupboard, a refrigerator, and a microwave oven. The walls are made of breeze-blocks with plaster. Several windows can be found in the right-hand wall. The walkways usually followed by the people are drawn on the figure.

Manuscript received May 14, 2003; accepted August 14, 2003. The editor coordinating the review of this paper and approving it for publication is M. Shafi. This work was supported by the French National Research Network in Telecommunications under the COMMINDOR Project. Part of this work was presented at the IEEE VTC, Jeju, Korea, April 22–25, 2003.

The authors are with the Institute of Electronics and Telecommunications of Rennes, Rennes 35043, France.

Digital Object Identifier 10.1109/TWC.2004.837276

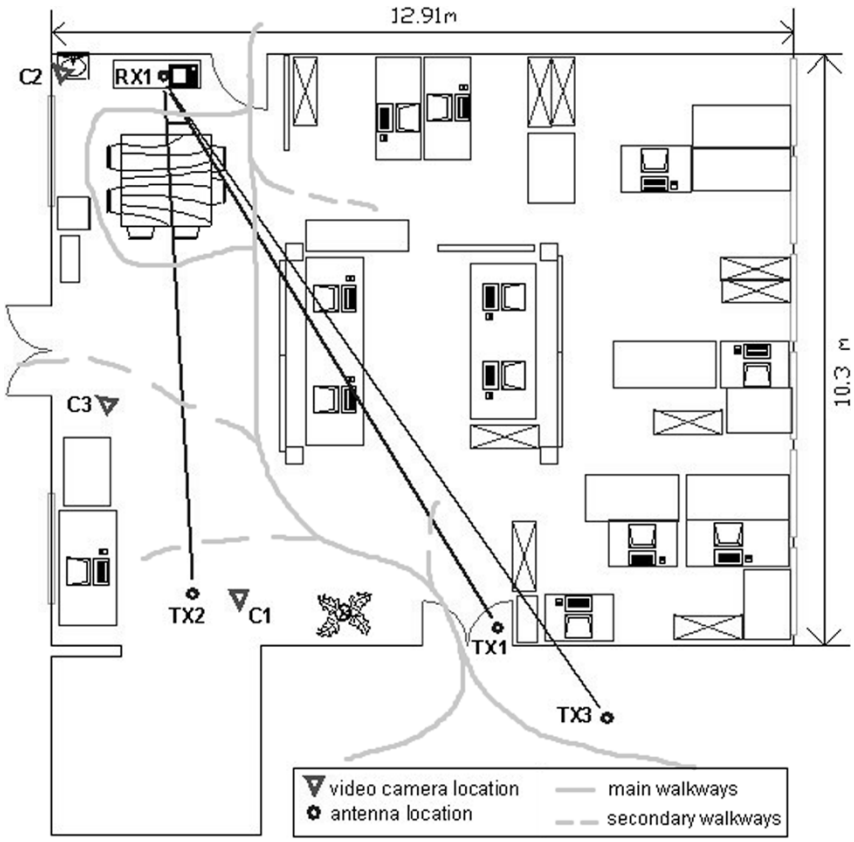

Fig. 1. Measurement site: laboratory.

C. Measurement Procedure

One receiving position (RX1) and three transmitting positions (TX1, TX2, and TX3) were chosen. RX was placed on the cupboard, at a height of 1.55 m, near the table where the main activity took place. Two TX positions were chosen in line of sight (LOS): TX1 on a post at a height of 2.27 m to simulate a base-station-to-device link, and TX2 on a table, at a height of 1.28 m to simulate a device-to-device link. The TX3 position was chosen in an adjacent room, for a non-LOS situation (NLOS), at a height of 1.58 m. All these locations are indicated in Fig. 1. For TX1 and TX2 positions, RX and TX antennas were pointed toward each other thanks to a laser pointer. For TX3 position both antennas are pointed toward the door that separates the rooms. The antennas were fixed during the measurements.

Measurements were performed over 15 days. Almost each day, three 40-min-long measurements were recorded at three moments, corresponding to coffee breaks: around 10:00, 13:00, and 16:00. Each day, TX position and/or antennas configurations were changed. During the measurements, a video camera shot the scene. Three camera positions were chosen, labeled C1, C2, and C3 in Fig. 1. The analysis of the video tapes makes it possible to know how many persons were in the vicinity of the antennas. A varied human activity can be observed: between zero and 15 persons, sitting and moving around the table, coming in and going out. In this paper, we define the "human activity" by the number of persons who are present at a given time in the vicinity of the antennas. Table I shows the measurement durations and the human activity for each configuration. It can be noted that the averages of the human activity are quite the same for all configurations (three to five persons). Therefore, comparisons between each configuration can be meaningful.

TABLE I
MEASUREMENT DURATIONS AND HUMAN ACTIVITY

TX Position	Antennas	Total measurement duration	Human activity	Mean human activity
TX1	H-H	4.4 h	0-15 persons	4
($d = 10.8\ m$)[a]	P-H	3.3 h	0-13 persons	4
	P-P	2.7 h	0-12 persons	3
TX2	P-H	1.8 h	0-10 persons	5
($d = 8.7\ m$)[a]	P-P	3.1 h	0-10 persons	4
TX3	H-H	2.1 h	? [b]	? [b]
($d = 13.2\ m$)[a]	P-H	2.1 h	? [b]	? [b]

[a] d: TX-RX distance
[b] incomplete video recordings

III. MEASUREMENT PROCESSING

A. Propagation Characteristics

The channel sounder evaluates the complex IR of the channel: $h(\tau, t)$, where τ is the delay and t the time. From the IR, several propagation characteristics are computed.

To decrease the measurement noise level, all these propagation characteristics are smoothed in time by means of a sliding window containing nine temporal samples (12.8 ms). The median value within the sliding window is used to obtain the smoothed characteristics.

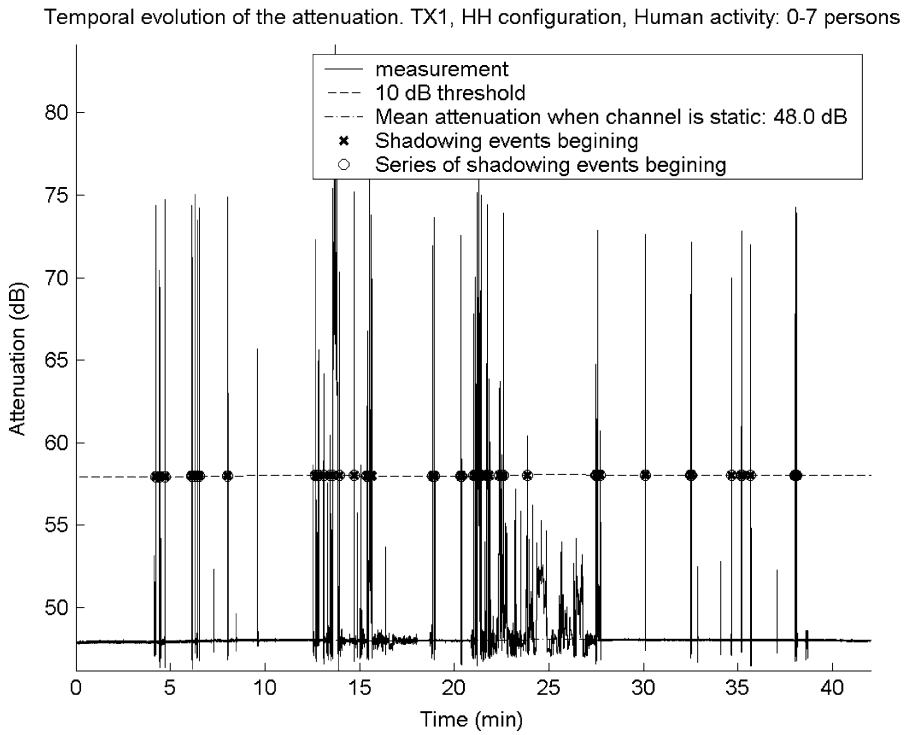

Fig. 2. Temporal evolution of the attenuation (TX1, HH configuration, zero to seven persons).

1) Attenuation: The attenuation $A(t)$ is the ratio of the transmitted power before the TX antenna on the received power after the RX antenna (the antennas are considered as part of the channel). The transmitted and received powers are computed on the whole signal bandwidth (500 MHz).

2) Temporal Fading: The temporal fading $F(t)$ is the temporal variation of the attenuation around a reference level A_{ref}

$$F(t)_{[\mathrm{dB}]} = A(t)_{[\mathrm{dB}]} - A_{\mathrm{ref}[\mathrm{dB}]}. \tag{1}$$

The reference level is measured before each long-term acquisition, when nobody is present. One can note that the median value of $A(t)$ is very close to the reference level.

3) Coherence Bandwidth: The coherence bandwidth is obtained from the autocorrelation function of the channel frequency response. The coherence bandwidth is computed for a threshold of 75% and is denoted Bc_{75}.

4) Delay Window: The X% delay window (DW_X), defined by ITU-R [12], is the temporal window containing X% of the IR power, so as the (100-X)% left are equally distributed around this window.

B. Shadowing Events

1) Definition: From the measurements, it can be observed that the attenuation strongly increases when the direct path is shadowed by a person. Fig. 2 shows a typical temporal evolution of the attenuation when people have a normal activity within the environement. A series of sharp attenuation peaks can be observed. These attenuation peaks are not uniformly distributed in time. This process is nonstationary because of people's movements.

For some of the measurements, these very fast variations are superimposed on slow variations that can be observed over several minutes. The standard deviation of these slow variations is not greater than 1 dB for LOS measurements, and not greater than 3 dB for NLOS measurements. The slow variations can be due to furniture manipulations or shadowing of indirect clusters of paths by a group of persons.

In NLOS situations, the standard deviation of the slow variations is greater than in LOS situation due to the absence of the direct path. The attenuation level is thus more sensitive to furniture displacements that create or destruct indirect paths.

These attenuation peaks caused by the human body can be characterized in amplitude and duration. For this characterization, we introduce the notion of "shadowing event" (SE). An SE is detected when $F(t)$ becomes greater than a threshold. We used four thresholds: 5, 10, 15, and 20 dB. The begining of an SE Tb_{SE} is the instant of a threshold crossing with a positive slope. The end of an SE Te_{SE} is the instant of a threshold crossing with a negative slope. To avoid taking into account small oscillations around the detection threshold, the calculation rules for Tb_{SE} and Te_{SE} are completed as follows. A threshold crossing with a positive (respectively negative) slope is considered as an SE beginning (end) if and only if the following criteria are met.

- The next crossing with a negative (positive) slope does not occur before nine temporal samples (i.e., 14.4 ms).
- The fading after the crossing above (under) the threshold is greater than one-tenth of the threshold (i.e., 0.5, 1, 1.5, or 2 dB).

Thanks to these conventions, the detected SEs globally fit with an intuitive detection of significant crossings. The SE's characteristics are defined as follows [Fig. 3(a)].

- Duration

$$D_{\mathrm{SE}} = Te_{\mathrm{SE}} - Tb_{\mathrm{SE}}. \tag{2}$$

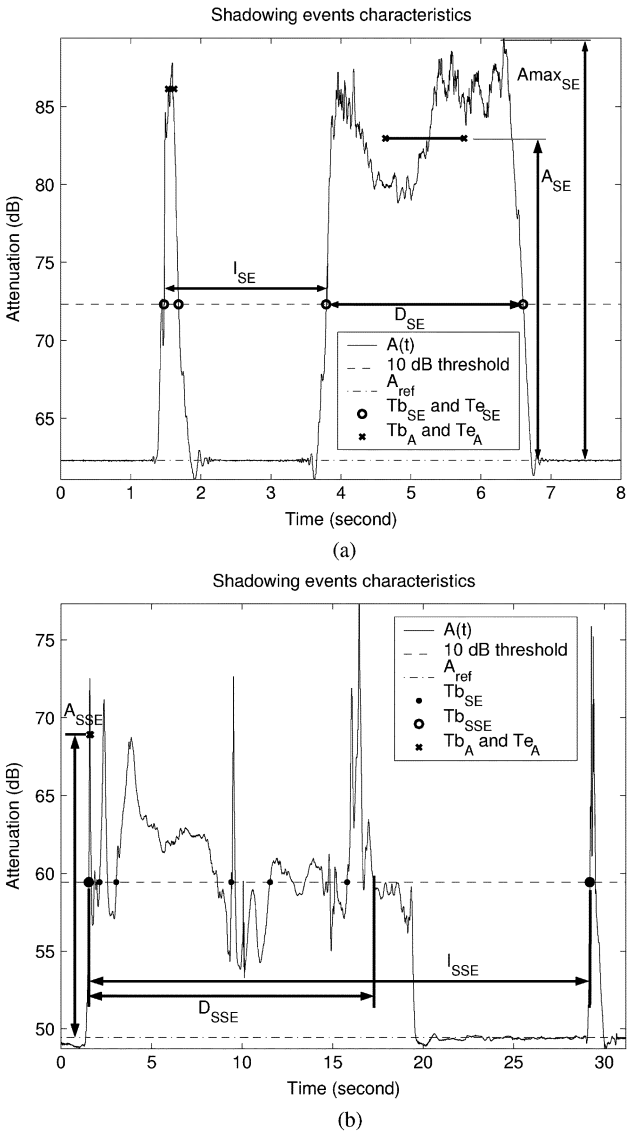

Fig. 3. (a) SE and and (b) SSE characteristics.

- Mean amplitude

$$A_{\mathrm{SE}} = \frac{3}{D_{\mathrm{SE}}} \int_{Tb_A}^{Te_A} F(t)\,\mathrm{d}t \tag{3}$$

where

$$Tb_A = Tb_{\mathrm{SE}} + \frac{D_{\mathrm{SE}}}{3} \quad \text{and} \quad Te_A = Te_{\mathrm{SE}} - \frac{D_{\mathrm{SE}}}{3} \tag{4}$$

and A_{SE} is an average over a time window centered on the middle of the SE. The width of this window is set to $D_{\mathrm{SE}}/3$ to eliminate the contribution of the lateral sides of the attenuation peak.

- Maximum amplitude

$$A\max_{\mathrm{SE}} = \max_{t\in[Tb_{\mathrm{SE}},Te_{\mathrm{SE}}]}[F(t)]. \tag{5}$$

- Pseudoperiod

$$I_{\mathrm{SE}}(n) = Tb_{\mathrm{SE}}(n+1) - Tb_{\mathrm{SE}}(n), \quad n \geq 1. \tag{6}$$

TABLE II
MEASUREMENT DURATION FOR EACH CONFIGURATION AND EACH HUMAN ACTIVITY RANGE

	0 pers.	1-5 pers.	6-10 pers.	11-15 pers.
HH1	55.2 min.	141.0 min.	62.2 min.	5.8 min.
PH1	33.0 min.	92.0 min.	56.4 min.	14.9 min.
PP1	22.7 min.	112.6 min.	21.9 min.	3.6 min.
PH2	8.2 min.	57.8 min.	43.4 min.	0.0 min.
PP2	26.5 min.	97.5 min.	64.1 min.	0.0 min.

TABLE III
N_{SE} CHARACTERISTICS FOR ALL CONFIGURATIONS[a]

	median of N_{SE}	$P_{\%}(N_{SE} > 1)$	$P_{\%}(N_{SE} > 5)$
HH1	1	30.8%	3.5%
PH1	1	19.4%	2.0%
PP1	1	45.9%	5.5%
PH2	1	29.0%	2.9%
PP2	1	32.9%	4.8%
HH3	1	47.3%	10.8%
PH3	2	50.8%	14.8%

[a] All activity ranges and all thresholds are joined

- Rising time $\mathrm{RT}_{\mathrm{SE}}$ is the time necessary for a 10 dB increase of the attenuation. $\mathrm{RT}_{\mathrm{SE}}$ is computed from the time between the crossing instant of $A_{\mathrm{ref}}+1$ dB and Tb_{SE}. This time is then related to a 10 dB increase.

It can be noted that the level crossing rate (LCR) [13], usually computed to characterize channel temporal variations, closely corresponds to the number of SEs per second. Also note that the average duration of fades (ADF) corresponds to the average of the SE duration. We do not use LCR and ADF in this paper because they are not suitable for the 60 GHz temporal variations. The major reason is that the distributions of the 60 GHz temporal characteristics are far from being symmetrical in relation to their mean (see Section IV-B2 for exemple). Mean values are thus not very representative of the "average behavior" of the distributions. We prefer to use median values.

2) Series of Shadowing Events: The duration between several successive SEs can be very short. These close SEs are generally caused by the movement of only one person between the antennas, as we noticed thanks to the video recordings. Moreover, the attenuation often stays greater than the reference level between two close SEs. This observation suggests that these SEs are, in a way, "correlated." In Fig. 3(b), the propagation channel is affected by a "shadowing phenomenon" from 1 up to 20 s. To characterize this phenomenon, we define the notion of "series of shadowing events" (SSEs). Two successive SEs, numbered n and $n+1$, belong to the same SSE if one of the following criteria is verified:

$$Tb_{\mathrm{SE}}(n+1) - Te_{\mathrm{SE}}(n) < t_{\max} \tag{7}$$

$$\min_{t\in\Omega}[A(t)] > A_{\mathrm{ref}} + A_{\mathrm{margin}}$$

$$\Omega = [Te_{\mathrm{SE}}(n), Tb_{\mathrm{SE}}(n+1)]. \tag{8}$$

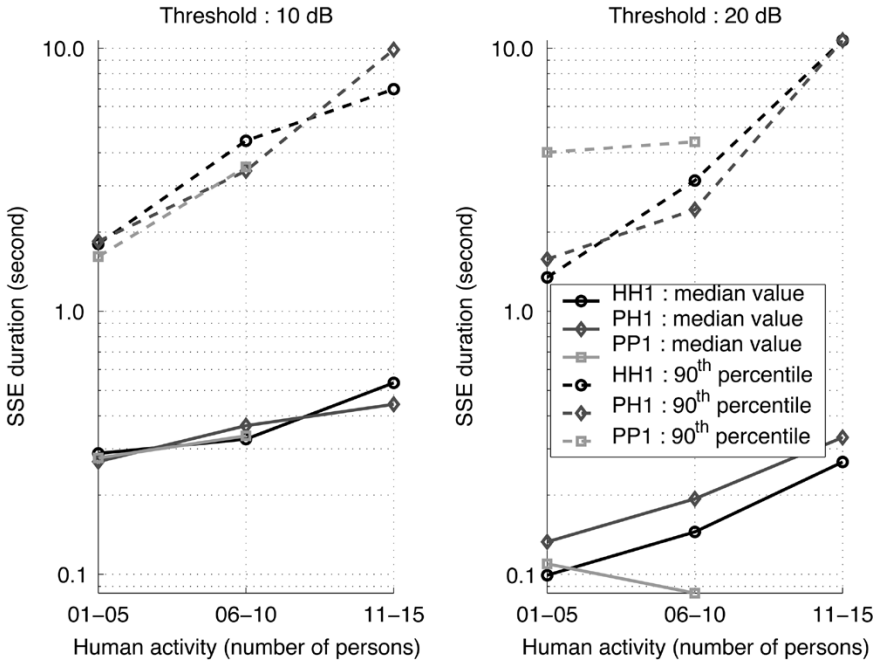

Fig. 4. Variations of the SSE duration for the TX1 configurations.

After some adjustments, $t_{\max}$ is set to 1.5 s, and A_{margin} to 1 dB. Thanks to these definitions, an SSE matches the physical interaction between a person and a wave path, as can be seen on the video recordings, and on the plots of the temporal variations of the attenuation. The SSE characteristics are the following [Fig. 3(b)].

- Number of SE per SSE N_{SE}.
- Begining and the end of the SEE

$$Tb_{\text{SSE}} = Tb_{\text{SE}}(1) \quad Te_{\text{SSE}} = Te_{\text{SE}}(N_{\text{SE}}). \tag{9}$$

- SSE duration

$$D_{\text{SSE}} = Te_{\text{SSE}} - Tb_{\text{SSE}}. \tag{10}$$

- SSE amplitude

$$A_{\text{SSE}} = \max_{1 \le n \le N_{\text{SE}}} \{A_{\text{SE}}(n)\}. \tag{11}$$

- SSE pseudoperiod

$$I_{\text{SSE}}(n) = Tb_{\text{SSE}}(n+1) - Tb_{\text{SSE}}(n), \quad n \ge 1. \tag{12}$$

- SSE rising time

$$\text{RT}_{\text{SSE}} = \text{RT}_{\text{SE}}(1). \tag{13}$$

IV. Results and Discussion

A. General Observations

Several parameters are taken into account in the above definitions: the detection threshold, the antenna configuration, the TX position, and the human activity. This activity is quantified by the number of persons who are present in the vicinity and between the antennas. This number was obtained by the analysis of the video recordings. As it is impossible to collect enough data for each number of persons from a natural activity, our analysis. focuses on the following activity ranges: 0, 1 to 5, 6 to 10, and 11 to 15 persons. The measurement files are split up into several parts corresponding to each human activity range. For each TX position and each antenna configuration, all the parts of measurement for one activity range are analyzed together. Table II shows the available duration of each activity range for all measurement configurations. The number of persons was sometimes greater than ten only for the TX1 position. But the observation durations were short (less than 15 min). The corresponding results are thus only indicative. For the PP1 configuration, less than ten SEs have been detected for this activity range, so we do not show the results in the following figures. For TX3 location, some video recordings were unfortunately incomplete.

In LOS situations (TX1 and TX2) the delay spread was short ($\text{DW}_{90} \le 5$ ns). The direct path conveyed most of the IR energy. For TX3 (NLOS), the IR was generally constituted by two main paths, and DW_{90} was about 20 ns.

B. SSE Characteristics

1) Number of SEs Per SSE (N_{SE}): When shadowing events occur in groups, they are considered as a "series of shadowing events" (see the above definitions). Several explanations can be provided: persons can follow one behind the other, one person can walk along the direct path, one person can stay quasi-static in the vicinity of one antenna, etc. All these situations conduct to fast variations in the multipath characteristics. The median number of SEs per SSE (N_{SE}) is always equal to one, except for two configurations (PP1, 6–10 persons, and PH3). This means that people's movements generally cause a simple SE. However, the percentage of SSEs composed of more than one SE, $P_{\%}(N_{\text{SE}} > 1)$, increases with the human activity. For HH1, $P_{\%}(N_{\text{SE}} > 1)$ lies from 25% for 1–5 persons up to 50% for 11–15 persons. When persons are numerous in an environment,

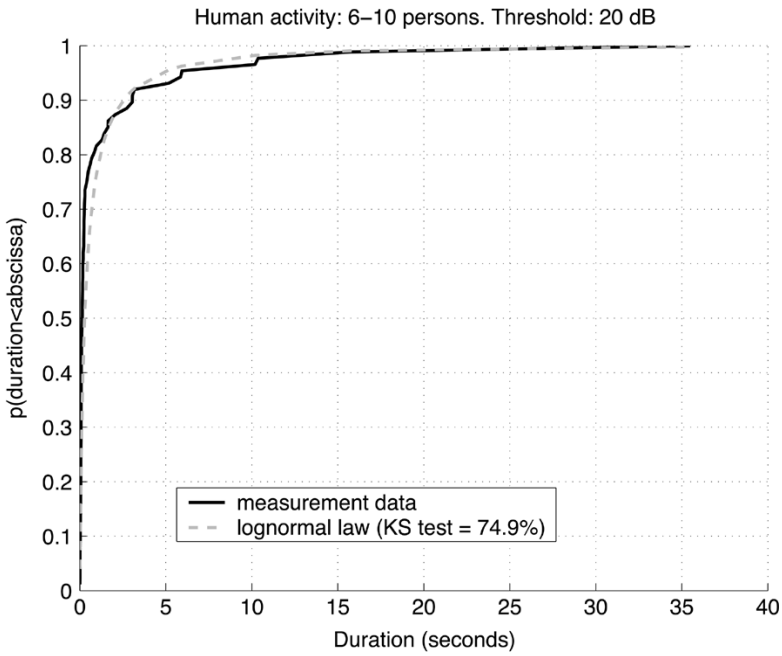

Fig. 5. CDF of the SSE durations for the HH1 configuration. Human activity: six to ten persons. Threshold: 20 dB.

they are more likely to move together, entailing closer SEs than when few people are present.

The detection threshold has no significant influence on N_{SE}.

N_{SE} also depends on the antennas configurations and on the visibility situation (Table III). N_{SE} is greater for the PP1 configuration due to the antennas beamwidth. Indirect paths with different angles of arrival are involved in the shadowing phenomenon. These paths are not always obstructed at the same time, which causes more variations of the received power, and therefore more detections of close SEs. For the other antennas configurations, the horn antenna confines the influence of the human activity within the channel to the direct path vicinity. All paths are shadowed together and thus more single SEs are detected.

For the TX3 location, about 50% of the SSEs are composed of more than one SE. This is due to the NLOS situation. There is no dominant path. Thus, paths reflected on the human bodies can combine with others in a destructive (or constructive) way, producing fast variations of the received power, and therefore more SE's detections.

These observations are confirmed by $P_{\%}(N_{\mathrm{SE}} > 5)$, which is greater for PP configurations (5.5% and 4.8%) and for the TX3 configurations (10.8% and 14.8%).

2) Duration (D_{SSE}): Fig. 4 shows that there is no clear dependence of the SSE's duration upon the antennas configuration. The SSE duration increases roughly linearly (on the logarithm scale) with the human activity. This behavior can be explained by the combining of individual actions, increasing the number of SEs per SSE and therefore the SSE duration. The detection threshold obviously influences the SSE duration. The following "key figures" can be remembered for the median duration:

- for a 10 dB threshold: 300 ms for one to five persons, 350 ms for six to ten persons, and 450 ms for 11 to 15 persons;
- for a 20 dB threshold: 100 ms for one to five persons, 150 ms for six to ten persons, and 300 ms for 11 to 15 persons.

TABLE IV
STATISTICS OF D_{SSE} FOR THE 10 dB THRESHOLD[a]

	N_{SSE}	Median value (s)	P90 (s)	P95 (s)
HH1	373	0.301	2.405	5.407
PH1	200	0.266	2.186	5.968
PP1	256	0.282	2.513	5.294
PH2	156	0.430	3.709	15.665
PP2	136	0.163	2.088	12.256
HH3	140	0.432	5.502	9.612
PH3	172	0.398	2.400	4.936

[a] All activity ranges are joined

The ninetieth percentiles of the SSE duration complete these figures and underscore the spread of the D_{SSE} values. More than a decade separates the median values from the ninetieth percentiles.

The cumulative distribution functions (cdfs) of the SSE durations have been fitted with different statistic laws, using the Kolmogorov–Smirnov test. Each time, the lognormal law best fits with the measurement data. The Weibull distribution sometimes gives good results. Fig. 5 shows the cdf of D_{SSE} for HH1, an activity of six to ten persons, and a 20 dB threshold. The fitted lognormal law is also plotted.

Comparisons between TX configurations are possible only for the global human activity (0–15 persons). Table IV presents the median values, the ninetieth and the ninety-fifth percentiles (P90 and P95) of D_{SSE} for each configuration and for the 10 dB threshold. The mean values are not presented because the spread of the durations is so wide that the mean values are not very significant. The number of SSEs N_{SSE} is also shown in Table IV to give an overview of the available data sample.

One can notice that the median values for TX1 are close to the "key figure" already reported above: 300 ms for an activity

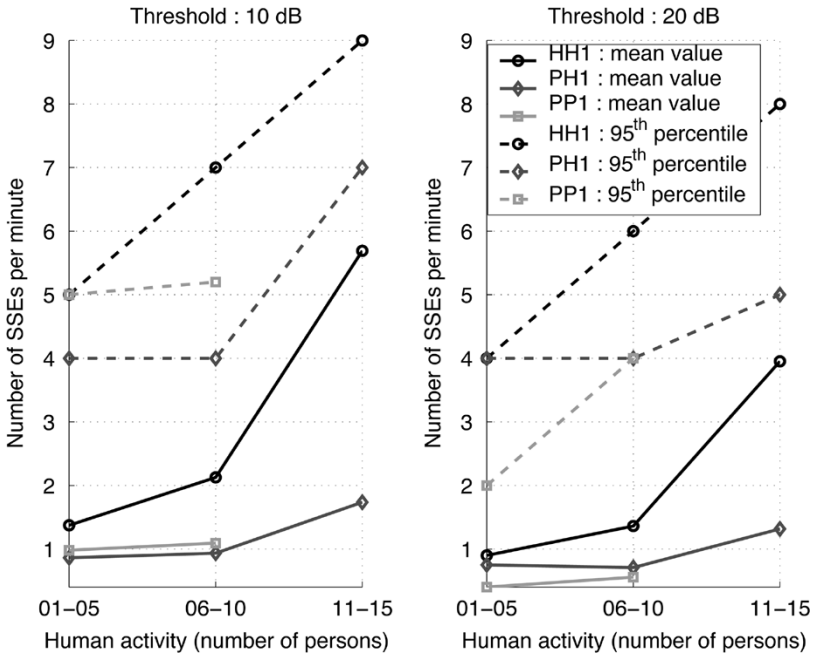

Fig. 6. Number of SSEs per minute for the TX1 configurations.

range for one to five persons. This observation is normal since the mean human activity within the channel was three to four persons for the three TX1 configurations (Table I).

The median duration is greater for NLOS configurations (TX3): around 400 ms. The same explanation as about N_{SE} can be supplied. The wave propagation is much more sensitive to people's movement when there is no direct path. More fast variations can be observed on the attenuation, which find expression in more SE detections within SSEs and longer SSEs.

PP2 is a special case for which the angular diversity is particularly important. Indirect paths with different angles of arrival can partly balance the direct path shadowing. Therefore, a strong obstruction can not be achieved except for a short time.

The "worst cases" (P95) are greater for the TX2 configurations (more than 10 s). The TX2 location can explain this result (Fig. 1): the direct path directly passed above the table at a height of about 1.50 m. The main activity took place around the table and this activity was "slow" (persons often stayed still for a while to chat).

3) Amplitude (A_{SSE})*:* The results show that the SSE amplitudes do not depend on the human activity. The mean SSE amplitudes differ only from a maximum of 2 dB between an activity of one to five persons and an activity of more than 11 persons. Table V shows the statistics of the SSE amplitudes for each antenna configuration, and for the 5 dB threshold. These values are extracted from the whole set of measurements (all activity ranges are joined).

For LOS situations, the mean and median values of A_{SSE} are greater than 15 dB if a directive antenna is used (HH1, PH1, and PH2).

For PP configurations (PP1 and PP2), the antenna beamwidth leads to lower amplitudes (mean and median values are less than 15 dB). The angular spread of the paths restricts the possibilities of complete obstruction, and thus reduces the SSE amplitude.

TABLE V
STATISTICS OF A_{SSE} FOR THE 5 dB THRESHOLD[a]

	Mean value (dB)	Median value (dB)	90^{th} percentile (dB)
HH1	15.5	16.6	22.9
PH1	19.8	21.3	25.1
PP1	12.2	11.9	18.6
PH2	18.1	18.9	23.6
PP2	9.0	8.7	12.1
HH3	12.0	9.9	22.8
PH3	11.6	12.4	15.6

[a] All activity ranges are joined

This is particularly true for PP2, which completes the previous remark about the duration.

For NLOS situations (TX3), the received power is low. The measurement dynamic thus interfered in the amplitude evaluation. So, for PH3, the measurement noise prevented detection of 20 dB threshold crossings. Globally, the attenuation fluctuations are more irregular in NLOS, and so there are more SSEs with a low amplitude.

4) Pseudoperiod (I_{SSE})*:* I_{SSE} spreads from about 2 s up to 20 min. This characteristic is highly dependent on the human activity, and it is difficult to highlight other dependencies. I_{SSE} logically decreases when the human activity increases. The wide spread of I_{SSE} and the observation of long-term variations of $A(t)$ (Fig. 2) suggest that SSEs also occur in series or "burst." This behavior is totally dependent upon the human activity.

The Kolmogorov–Smirnov test leads one to conclude that the cdfs of I_{SSE} follow lognormal laws. I_{SSE} is an interesting characteristic for modelization purpose. These considerations will be developped in further works. For the phenomenon description, however, we prefer to present the instantaneous SSE rate:

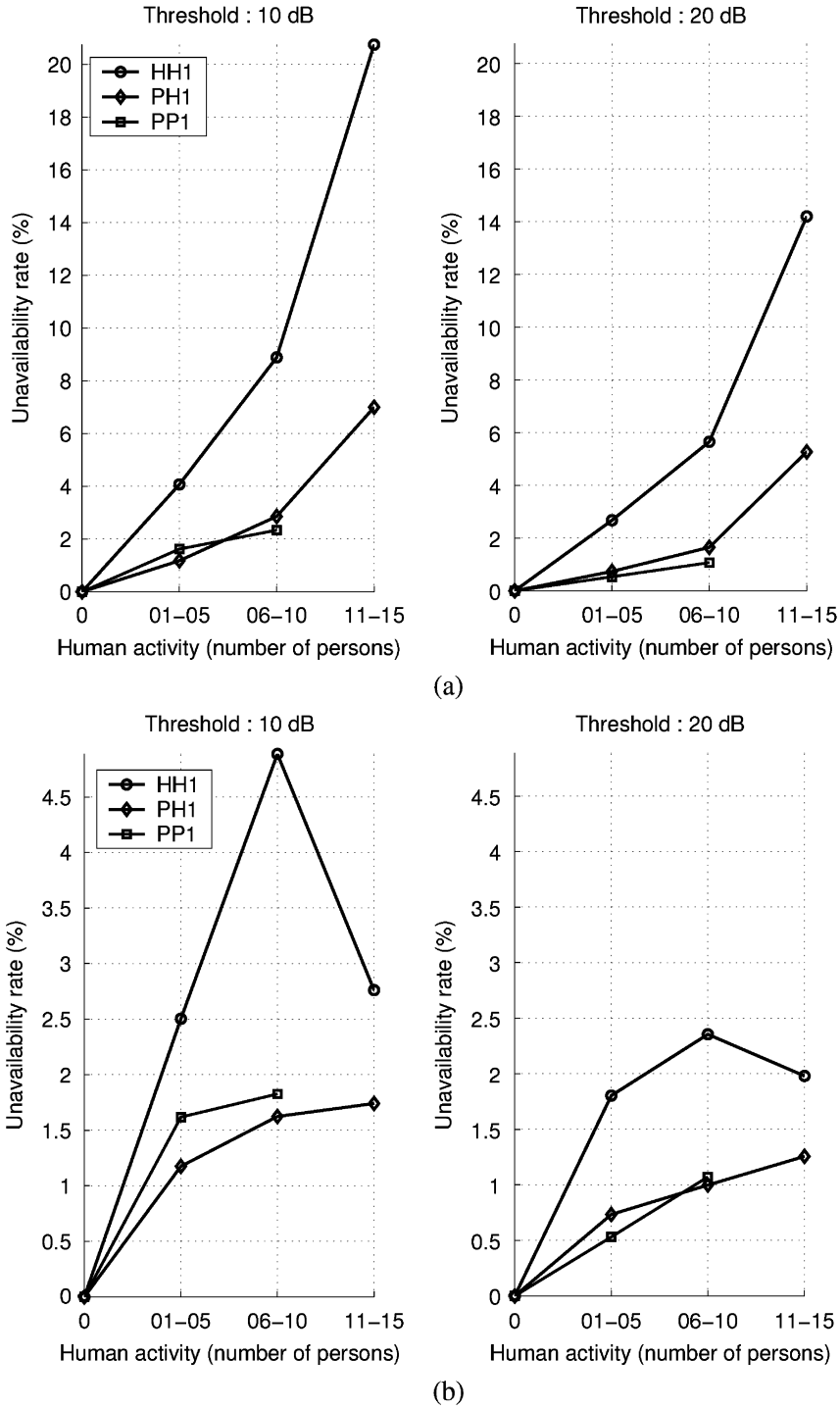

Fig. 7. Unprocessed and corrected unavailability rates for TX1 and for the 10- and 20-dB thresholds. (a) Unprocessed and (b) corrected UR.

$R_{\mathrm{SSE}}(t)$, which is the temporal variation of the number of SSE's per minute. This parameter is computed over the measurement duration by means of a sliding window. The duration of the window is 1 min. The window is slided with a step of 1 s. The spread of the R_{SSE} values is limited and the statistics are more significant.

Fig. 6 shows the statistics of R_{SSE} for the TX1 configurations. The average SSE rate globally varies from one up to two SSEs per minute for a 10 dB threshold, and from 0.5 up to 1.5 SSEs per minute for a 20 dB threshold. For all activities joined, the average number of SSEs per minute is about one, and P95 is about five SSEs per minute. The other configurations do not reveal significant differences except for PP2: average shadowing rate of 0.5 SSE per minute and a ninety-fifth percentile of only three SSEs per minute (for a 10 dB threshold). This particular position and the use of two patches contribute to reduce the rate of the shadowing phenomenon.

5) Rising Time (RT_{SSE})*:* The SSE rising time does not depend on the human activity. This is an obvious result since the parameter is directly linked with the velocity of the persons

TABLE VI
SSE RISING TIMES FOR EACH ANTENNA CONFIGURATION

	median (ms)	P10 (ms)	P5 (ms)
HH1	93	42	34
PH1	62	33	27
PP1	136	60	43
PH2	96	38	25
PP2	197	59	34
HH3	111	33	24
PH3	154	37	33

TABLE VII
UNAVAILABILITY RATES OF THE CHANNEL FOR ALL CONFIGURATIONS (THRESHOLD: 10 dB)

	unprocessed UR	corrected UR
HH1	5.7%	4.0%
PH1	1.9%	1.6%
PP1	1.9%	1.7%
PH2	6.8%	5.2%
PP2	1.8%	1.8%
HH3	4.7%	3.1%
PH3	3.0%	3.0%

within the channel. The results are then presented for all activity ranges joined. Table VI shows three statistics of $\mathrm{RT}_{\mathrm{SSE}}$ for each antenna configuration: the median value and the tenth and the fifth percentiles (P10 and P5). These values are computed for the SSEs detected with a threshold of 15 dB (PH2, PP2, HH3, and PH3) or 20 dB (HH1, PH1, and PP1).

The rising time can be short. Globally, in 5% of the cases, the attenuation increases of 10 dB in less than 30 ms. For NLOS situations, the median rising time is longer than for LOS situations and the same antenna configurations. One can notice that the difference between all configurations tends to diminish for the "worst cases" (P5).

C. Unavailability Rate of the Channel

One can reasonably think that the channel becomes unavailable during a series of shadowing events. The same observation is reported in [14] for 40 GHz radio links. From a viewpoint of a communication system, the shadowing events have three problematic characteristics: the fading rising time is short, the fading duration is long, and the fading amplitude is strong. The techniques used to overcome the channel temporal variations will probably be inefficient in the case of deep and long temporal variations of the 60 GHz channel. This means that every commnication could easily be interrupted during a shadowing event. From the measurements, an "unavailability rate" (UR) of the channel is defined as the sum of the SSE durations divided by the total measurement duration

$$\mathrm{UR} = \frac{\sum_{i=1}^{N_{\mathrm{SSE}}} D_{\mathrm{SSE}}(i)}{T_{\mathrm{meas}}}. \tag{14}$$

It is important to notice that this UR is highly dependent on the hazard of the human activity. A person can walk, stop on the direct path, and stay during a very long time. Of the SSEs, 3.5% last more than 10 s and 1.0% more than 30 s. These very long SSEs can be seen as "outliers," and they have a strong impact on the UR. As these outliers are not uniformly distributed between the antenna configurations and the human activity ranges, and as the observation times are not the same for all configurations, the comparisons might be distorted. A corrected UR is then computed so as each SSE with a duration that represents more than 0.5% of the total measurement duration, is not taken into account in the UR calculation. This convention is partly arbitrary but allows a more trimmed UR estimation and more significant comparisons between antennas configurations.

Fig. 7 shows the variation of the unprocessed and the corrected unavailability rates with the human activity. The UR logically increases with the human activity. The corrected UR values are low for an activity of 11 to 15 persons because the observation durations are too short. For this case, more realistic values would lie between the corrected UR and the unprocessed UR.

One can underscore the effect of the antennas: patch antennas can benefit from an angular diversity. Table VII shows the URs for all configurations, and all activity ranges joined. The corrected UR can vary from 1.7% up to 5.2% depending on the configurations. The PH1, PP1, and PP2 configurations present very close URs (1.6%–1.9%). The channel is less available for the HH1 and PH2 configurations.

D. Wide-Band Characteristics

Wide-band characteristics can complete the above observations. We focus here on the 75% coherence bandwidth (Bc_{75}). An important correlation can be found between the temporal fading and the variation of Bc_{75} (Bc_{75} decreases when the fading amplitude inscreases). This can partly be explained by the noise level: the received power during a SE can be close to the noise level (especially for PP configurations), which influences the Bc_{75} computation. For HH1 configuration however, even when the fading amplitude is greater than 20 dB, Bc_{75} is greater than 250 MHz during 29.8% of the time.

The cdfs of Bc_{75} reveal a virtually "on–off" behavior: Bc_{75} is less than 50 MHz or more than 250 MHz. The middle values are very few. Therefore, Bc_{75} can be used to estimate the channel unavailability. Fig. 8 shows the probability that Bc_{75} is less than 50 MHz for the three antenna configurations.

V. CONCLUSION

This paper presents the main results of several measurement campaigns of the 60 GHz propagation for a time-varying channel. The temporal variations of the channel are caused by people's movements while antennas are fixed. Some new definitions ("shadowing event" and "series of shadowing events") are introduced to quantify the impact of human activity on propagation characteristics.

The results confirm that human bodies are significant obstacles (and reflectors) for the millimeter-waves propagation. The movements within the channel cause a problematic "shadowing effect," especially when the direct path is obstructed.

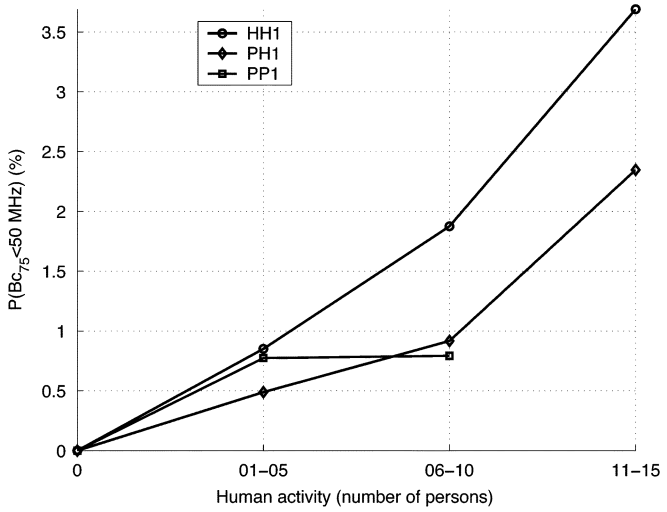

Fig. 8. Probability that the 75% coherence bandwidth is less than 50 MHz.

The duration of this shadowing effect is very long (most of the time several hundreds of milliseconds) compared to the symbol duration of high data rate systems. This duration increases with the number of persons within the environment. On the other hand, the amplitude of the shadowing effect do not depend on the number of persons but on the antennas configurations. When the antennas are too directive to introduce angular diversity, the mean amplitude is greater than 15 dB, and in 10% of the cases, this amplitude is greater than 20 dB.

The shadowing effect is globally less severe (shorter duration, lower amplitude and slower rising time) if the antenna beamwidths are large enough to introduce an angular diversity both in transmission and in reception. These results lead to consider that the channel is unavailable during about 1–2% of the time when one to five persons move between the antennas or in their vicinity.

These results are interesting for modelization purposes. The statistical distributions of the SSE characteristics (duration, amplitude, pseudoperiod, and rising time) make it possible to generate realistic "temporal shapes" that simulate the temporal variations of the attenuation.

High data rate networks need to take into account the influence of the human activity. Some solutions have been suggested by different authors. All these solutions take advantage of a sort of diversity. An access point diversity is often proposed [9], [10]. A disadvantage of such solutions is the amount of cabling and others network deployment considerations. For some applications, especially for general public, such solutions cannot be implemented.

Previous measurement campaigns revealed that the main angles of arrival in the azimuthal plan spread over 360° [15]. This can be used to overcome the shadowing events. Actually, when a direction of arrival is obstructed by a human body, others are likely to be free. Multisector antennas associated with switching or combining systems must be developed to take advantage of this angular diversity. Moreover, if a device within the wireless network can be used for relaying the communications between two others, a sort of site diversity is added and obstruction problems are reduced again. The network deployment is simplified (ad hoc network approach) but, on the other hand, the modem complexity increases. The results of this paper, extracted from propagation measurements, can be helpful for the design of these future communications systems.

ACKNOWLEDGMENT

The authors thank S. Ammoun from the Lebanese University for his active contribution to the work reported in this paper, particularly for the preparation and the realization of the measurement campaign.

REFERENCES

[1] S. Ohmori, Y. Yamao, and N. Nakajima, "The future generations of mobile communications based on broadband access technologies," *IEEE Commun. Mag.*, pp. 134–142, Dec. 2000.

[2] T. Manabe, Y. Miura, and T. Ihara, "Effects of antenna directivity and polarization on indoor multipath propagation characteristics at 60 GHz," *IEEE J. Select. Areas Commun.*, vol. 14, pp. 441–448, Apr. 1996.

[3] J.-H. Park, Y. Kim, Y.-S. Hur, K. Lim, and K.-H. Kim, "Analysis of 60 GHz band indoor wireless channels with channel configurations," in *Proc. IEEE Int. Symp. Personal, Indoor, and Mobile Radio Communications (PIMRC'98)*, Boston, MA, Sept. 8–11, 1998, pp. 617–620.

[4] T. Manabe, K. Sato, H. Marsuzawa, K. Taira, T. Ihara, and Y. Kasashima, "Polarization dependence of multipath propagation and high-speed transmission characterisitics of indoor millimeter-wave channel at 60 GHz," *IEEE Trans. Veh. Technol.*, vol. 44, pp. 268–274, May 1995.

[5] H. Xu, V. Kukshya, and T. Rappaport, "Spatial and temporal characterization of 60 GHz indoor channels," *IEEE J. Select. Areas Commun.*, vol. 20, pp. 620–630, Apr. 2002.

[6] S. Guerin, C. Pradal, and P. Khalfa, "Indoor propagation narrow band and wide band measurements around 60 GHz using a network analyzer," in *EURO COST*, Apr. 1995.

[7] P. Marinier, G. Delisle, and C. Despins, "Temporal variations of the indoor wireless millimeter-wave channel," *IEEE Trans. Antennas Propagat.*, vol. 46, pp. 928–934, June 1998.

[8] S. Obayashi and J. Zander, "A body-shadowing model for indoor radio communication environments," *IEEE Trans. Antennas Propagat.*, vol. 46, pp. 920–927, June 1998.

[9] M. Flament and M. Unbehaum, "Impact of shadowing fading in a mm-wave band wireless network," in *Proc. Int. Symp. Wireless Personal Multimedia Communications (WPMC'2000)*, vol. 1, Bangkok, Thailand, Nov. 2000, pp. 427–432.

[10] K. Sato and T. Manabe, "Estimation of propagation-path visibility for indoor wireless LAN systems under shadowing condition by human bodies," in *Proc. IEEE Veh. Technol. Conf. (VTC'98)*, Ottawa, ON, Canada, May 1998, pp. 2109–2113.

[11] S. Guillouard, G. El Zein, and J. Citerne, "High time domain resolution indoor channel sounder for the 60 GHz band," in *Proc. Eur. Microwave Conf. (EMC'98)*, vol. 2, Amsterdam, The Netherlands, Oct. 1998, pp. 341–344.

[12] *Multipath Propagation and Parameterization of Its Characteristics*. International Telecommunication Union, Radiocommunication Sector (ITTU-R) Recommendation P.1407.

[13] T. Rappaport, *Wireless Communications: Principles and Practice*. Englewood Cliffs, NJ: Prentice-Hall, 1996, p. 185. sec. 4.7.3.

[14] R. Bultitude, R. Hahn, and R. Davies, "Propagation considerations for the design of an indoor broad-band communications system at EHF," *IEEE Trans. Veh. Technol.*, vol. 47, pp. 235–245, Feb. 1998.

[15] S. Collonge, G. Zaharia, and G. El Zein, "Wideband and dynamic characterization of the 60 GHz indoor radio propagation—Future home WLAN architectures," *Ann. Telecommun.*, vol. 58, no. 3–4, Mar.–Apr. 2003.

Sylvain Collonge received the M.Sc. and Ph.D. degrees in electronics and communications systems from the Institut National des Sciences Appliquees de Rennes (INSA), France, in 2000 and 2003, respectively.

He has been involved in the French RNRT project "Commindor," a feasibility study of low cost and high data rate communications in the 60 GHz band for domotic applications.

Gheorghe Zaharia received the B.S. degree in electronics and telecommunications from the Technical University (formerly Polytechnic Institute) of Iasi in 1981 and the D.E.A. and Ph.D. degrees in telecommunications—signal processing and electronics from the Institut National des Sciences Appliquees de Rennes (INSA), France, in 1991 and 1997, respectively.

Between 1983–1990 he was a Lecturer at the Technical University of Iasi. Between 1983–1985 he studied mathematics at University "Al. I. Cuza" of Iasi. Since 1997, he has been an Associate Professor in the Department of Electronics and Communications Systems Engineering, INSA. His teaching and research interests mainly concern the study of radiowaves propagation, information theory, and coding.

Ghais El Zein received the Ph.D. and Habilitation a Diriger des Recherches (HDR) degrees in telecommunications—signal processing and electronics from Rennes 1 University, France, in 1988 and 1998, respectively.

From 1985 to 1987, he was a Lecturer, and from 1990 to 1999, an Associate Professor, in the Department of Electronics and Communications Systems Engineering, Institut National des Sciences Appliquees de Rennes, where he is currently a Professor. His teaching and research interests mainly concern the study of radiowave propagation phenomena and the evaluation of their effects on communication systems performance. Since 2001, he has been the Assistant Director of the Institute of Electronics and Telecommunications of Rennes. He is a member of Commissions C and F of CNFRS-URSI and a member of COST 273.